

## 低空遥感平台下可见光与多光谱传感器在水稻纹枯病 病害评估中的效果对比研究

赵晓阳<sup>1,2</sup>, 张 建<sup>1,2\*</sup>, 张东彦<sup>3</sup>, 周新根<sup>4</sup>, 刘小辉<sup>3</sup>, 谢 静<sup>5\*</sup>

1. 华中农业大学资源与环境学院, 湖北 武汉 430070
2. 农业部长江中下游耕地保育重点实验室, 湖北 武汉 430070
3. 安徽大学安徽省农业生态大数据工程实验室, 安徽 合肥 230601
4. Texas A&M AgriLife Research and Extension Center, Beaumont, TX 77713, USA
5. 华中农业大学理学院, 湖北 武汉 430070

**摘 要** 高效无损地评估农作物病害等级, 对于实际农业生产和研究都具有重要意义。研究探讨了基于低空无人机遥感平台进行水稻纹枯病病害等级评估的可行性, 分析可见光与多光谱传感器的光谱响应差异及其对感病水稻光谱反射率获取的影响, 并定量对比两种传感器的病害监测效果。实验研究区由 67 个不同品种的水稻小区组成, 每块小区均分为相接的纹枯病接种区和侵染区。以大疆精灵 Phantom 3 Advanced 小型消费级无人机作为搭载平台, 分别搭载该无人机系统自带的可见光传感器和 MicasenseRedEdge™ 多光谱传感器获取遥感影像。同时, 通过植保专家现场调查的方式识别病害等级, 并利用 Trimble 公司的手持式 NDVI 测量仪获取实测 NDVI 值。基于影像拼接、波段叠合、辐射校正后的预处理结果, 对可见光图像的接种区和侵染区共 134 个小区计算七种可见光植被指数, 即 NDI(normalized difference index), ExG(excess green), ExR(excess red), ExG-ExR, B\*, G\*, R\*, 多光谱图像除上述可见光指数外再计算 NDVI(normalized difference vegetation index), RVI(ratio vegetation index)和 NDWI(normalized difference water Index)三种多光谱植被指数。将计算得到的图像植被指数与地面实测 NDVI 进行相关性分析, 以选取两种传感器的最优图像植被指数建立水稻纹枯病病害等级反演模型。相关性分析结果表明, 基于多光谱传感器计算的图像 NDVI 与实测 NDVI 拟合度最高, 接种区  $R^2$  为 0.914, RMSE 为 0.024, 侵染区  $R^2$  为 0.863, RMSE 为 0.024。对于可见光传感器, NDI 与实测 NDVI 的相关性最好, 接种区  $R^2$  为 0.875, RMSE 为 0.011, 侵染区  $R^2$  为 0.703, RMSE 为 0.014。比较两种传感器两种区域的同一图像植被指数与实测 NDVI 的一致性, 除 B\* 外, NDI, ExR, ExG-ExR, G\*, ExG, R\* 与实测 NDVI 基本属于高度相关, 在病害严重的接种区, 两种传感器对水稻纹枯病的监测效果相近, 但在病害相对较轻的侵染区, 多光谱传感器的监测更为精确灵敏。基于多光谱图像 NDVI 建立的病害等级反演模型,  $R^2$  达到 0.624, RMSE 为 0.801, 预测精度达到 90.04%, 模型效果良好。而基于可见光图像 NDI 建立的反演模型,  $R^2$  为 0.580, RMSE 为 0.847, 预测精度为 89.45%, 效果稍差。对比分析可见光与多光谱传感器的光谱响应曲线, 可见光传感器可获取可见光范围的红、绿、蓝三个波段, 波段范围互相重叠, 多光谱传感器包含五个成像单元, 可独立获取从可见光到近红外的五个窄波光谱波段, 提供更加准确的光谱信息。比较传感器获取的接种区和侵染区水稻平均反射率曲线得出, 多光谱传感器不仅在可见光波段反映了较可见光传感器更强的差异, 在红边和近红外波段差异则更加明显, 这说明专业窄波段传感器在病害监测方面较宽波段消费级传感器更有优势。综上所述, 基于可见光与多光谱传感器的低空无人机遥感平台进行水稻纹枯病病害等级评估是可行的, 多光谱传感器精确灵敏, 可用于纹枯病的早期监测, 可见光传感器效果稍差但经济易于推广。研究结果为病虫害防治提供决策支持, 有助于推动实现精准农业, 保障粮食安全。

收稿日期: 2018-01-15, 修订日期: 2018-05-20

基金项目: 国家自然科学基金项目(31501222, 41201364, 41771463), 中央高校基本科研业务费专项(2018JC012, 2017JC038, 2015BQ026, 2014JC008), 国家大学生创新训练项目(201610504017)资助

作者简介: 赵晓阳, 1996 年生, 华中农业大学资源与环境学院本科生 e-mail: xyzhao@webmail.hzau.edu.cn

\* 通讯联系人 e-mail: jz@mail.hzau.edu.cn; xiejing625@mail.hzau.edu.cn

关键词 多光谱传感器; 可见光传感器; 低空遥感; 水稻纹枯病; 病害等级评估; 植被指数

中图分类号: S127 文献标识码: A DOI: 10.3964/j.issn.1000-0593(2019)04-1192-07

## 引 言

水稻是全球约半数人口的主食,是世界贸易中受保护程度最高的粮食之一<sup>[1]</sup>。水稻纹枯病是降低水稻粮食品质,增加倒伏的主要原因,严重时可使产量减少 50%<sup>[2]</sup>。因此,有必要对水稻纹枯病进行实时、宏观、准确的监测和评估<sup>[3]</sup>。目前,农作物病虫害监测在数据采集上主要依靠植保人员田间取样的传统方式,存在以点代面的代表性差、主观性强和时效性差等弊端<sup>[4]</sup>。国内外学者利用地物光谱仪 ASDField-spec FR2500 对小麦、水稻、大豆、玉米等作物的病虫害胁迫进行了深入研究,但这种方式只可以对作物个体进行研究,采集的光谱信息是混合的,构建的反演模型精度受到限制<sup>[5]</sup>。航空航天遥感技术能够在较大范围内快速获取空间连续地表信息,RGB、多光谱、高光谱、荧光成像和热红外传感器已被广泛应用于识别植物病害症状并估计疾病的严重程度<sup>[6-8]</sup>。针对水稻纹枯病, Qin 等<sup>[9]</sup>利用宽波段高空间分辨率机载遥感影像数据,清晰地区分了中度和高度病害植被,提出在识别轻微感病植被时,需采用高光谱分辨率的影像。Zhang 等<sup>[2]</sup>发现当水稻纹枯病呈现出典型特征时,多光谱农业数码传感器 ADC 较 SPAD-502 而言,能更好的识别病害等级,同时测定了纹枯病的光谱敏感范围。Faranak 等<sup>[11]</sup>采用 SPOT5 图像检测纹枯病,提出利用植被指数 RVI14, SDI14 和 SDI24 可以较好的从感病植被中提取健康植被。近年来,搭载小型数字传感器的消费级无人机遥感平台越来越多的应用于农业中<sup>[11-12]</sup>,其运行维护成本低、高效、灵活性强、作业周期短,可弥补卫星遥感数据由于射程远而导致的精度不高和因为重访周期长而不能达到实时监测等缺点<sup>[6, 13-14]</sup>。已有少数病害研究基于无人机遥感平台展开, Sankaran 等<sup>[15]</sup>将多光谱和热红外成像仪集成于小型多旋翼无人机平台上,有效地监测了柑橘黄龙病,而基于无人机平台的水稻病害等级评估还处于起步阶段。

为探讨消费级无人机常用载荷在水稻病害等级评估中的可行性,本研究以感染纹枯病的 67 种不同品种的水稻为观测对象,基于小型消费级无人机,分别搭载普通传感器和多光谱传感器获取水稻田间影像,同时在地面同步测量了田间 NDVI 值、病害指数。定量地评估基于不同传感器图像多种植被指数与实测 NDVI 之间的相关性,并利用图像上最优植被指数反演水稻纹枯病病害指数。

## 1 实验部分

### 1.1 研究区

本研究的试验地点位于德克萨斯州博蒙特市西部的美国德州农工大学 AgriLife 研究与推广中心的试验田(30°03'53.4"N, 94°17'38.7"W)。试验以接种了纹枯病的 67 个不同品种的水稻为研究对象,供试品种有非常敏感纹枯病的

CL111, Cocodrie, Presidio, Antonio 和 Colorado; 易感病害的 CL151, Jupiter, Cheniere, Jazzman-2, CL152 和 Rex; 中度敏感病害的 CL271, Della2 和 Rondo 等。水稻于 2015 年 4 月 15 日播种,于拔节期进行病菌接种。每个试验小区长 7 m,宽 4 m,平均分成两部分,一部分为接种区,另一部分为潜在侵染区,用于观察纹枯病的侵染速度和程度。由于试验品种抗性不同、生长阶段不同,水稻纹枯病病害程度也不同。通过专家现场调查的方式,人工识别水稻病害程度,其中病害严重程度分为 0—9 级,数值越大,表示病害越严重(图 1)。

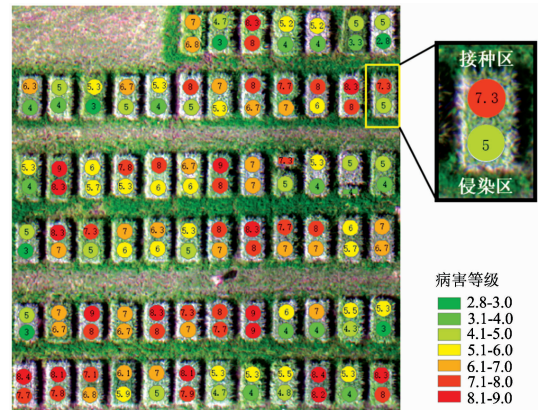


图 1 研究区

Fig. 1 Study area

### 1.2 数据获取

本研究设计的无人机系统由大疆创新科技有限公司的大疆精灵 Phantom 3 Advanced 小型消费级无人机作为搭载平台,分别搭载该无人机系统自带的可见光传感器[图 2(a)]和美国 Micasense 公司的 Micasense RedEdge™ 多光谱传感器[图 2(b)]。实验于 2015 年 8 月 30 号 10 点至 13 点之间展开,无人机飞行高度均为 42 m,针对水稻实验样区进行成像,其中可见光传感器为分辨率 4 000×3 000,以 DNG 24bit 格式记录,多光谱传感器为分辨率 1 280×960,以 TIFF 16 bit 格式记录,两种图像格式均为无损压缩方式存储。使用美国 Trimble 公司的手持式 NDVI 测量仪(GreenSeeker® Handheld Crop Sensor)[图 2(c)],同步测量各个田块接种区和侵染区的 NDVI 值。

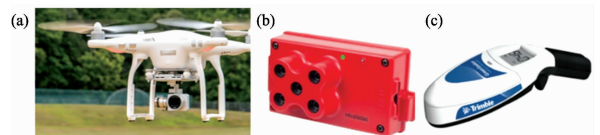


图 2 (a) 小型无人机及可见光传感器; (b) 多光谱传感器; (c) 手持式 NDVI 地面测量仪  
Fig. 2 (a) Small UAV and visible light sensor; (b) Multispectral sensor; (c) Handheld crop sensor

1.3 数据处理与分析

图像分析前需要经过影像拼接、波段叠合、辐射校正。图 3 是图像预处理结果。

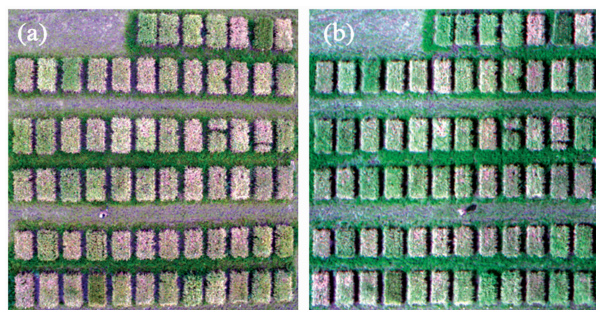


图 3 (a) 可见光图像; (b) 多光谱真彩色 b-321 合成图像  
Fig. 3 (a) Visible light image; (b) Multispectral true color b-321 composite image

两种传感器光谱响应曲线和 67 种感病水稻平均反射率曲线如图 4 所示。若使用消费级传感器的自动曝光模式成像,受环境影响成像参数不固定,无法将不同波段不同位置的图像信息在同一标准下进行比较。因此,本研究采用手动设置模式人为设定曝光时间/快门速度、光圈和 ISO 速度,但参数的设置是以成像清晰为前提,所以会存在像素值较饱

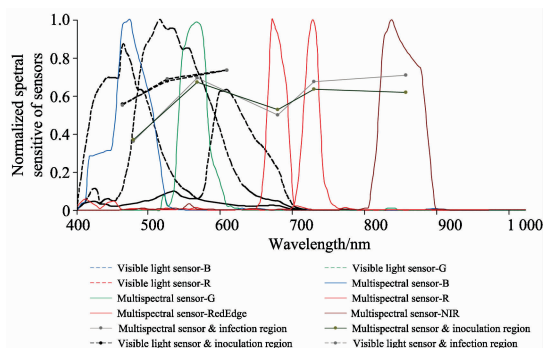


图 4 传感器光谱响应曲线与感病水稻光谱曲线  
右轴: 水稻纹枯病光谱曲线刻度

Fig. 4 Spectral response curves of sensors and spectral curves of rice with ShB

Note: the right axis is the scale of spectral curve of rice with ShB

表 1 可见光和多光谱传感器植被指数

Table 1 Vegetation Indices of visible light and multispectral sensor

Type	Vegetation indices <sup>[15]</sup>		Sensor	
	Model		Visible light	Multispectral
Multispectral indices	Normalized Difference Vegetation Index(NDVI) = (NIR - R) / (NIR + R)		×	√
	Ratio Vegetation Index(RVI) = NIR/R		×	√
	Normalized Difference Water Index(NDWI) = (G - NIR) / (G + NIR)		×	√
	B* = B / (B + G + R)		√	√
	R* = R / (B + G + R)		√	√
Visible light indices	G* = G / (B + G + R)		√	√
	Excess Green(ExG) = 2G* - R* - B*		√	√
	Excess Red(ExR) = 1.4R* - G*		√	√
	ExG-ExR		√	√
	Normalized Difference Index(NDI) = (G - R) / (G + R)		√	√

和的情况,这使得感病水稻反射率整体拉伸较实际值偏高。但这并不影响后续分析,因为本研究使用的植被指数均为比值指数,可在很大程度上消除反射率整体拉伸造成的影响,以及太阳光照差异、云阴影、部分大气衰减和部分地形差异的噪声影响。

可见光传感器可以获取可见光范围的红、绿、蓝三个波段,波段范围互相重叠。多光谱传感器包含五个成像单元,可以独立获取从可见光到近红外的五个窄波光谱波段,提供更多更加准确的水稻长势信息。水稻感染立枯丝核菌后内部结构发生变化,特别是叶绿素等色素浓度或含量的下降,使得叶绿素在蓝、红波段的吸收变弱,反射增强。图 4 也表明,可见光传感器获取的接种区水稻反射率曲线较侵染区而言,蓝光、红光反射率略微升高,绿光略微降低,符合实际情况,但两者间无显著差异。多光谱传感器获取的感病水稻反射率曲线,接种区蓝光、红光反射率升高,绿光、红边、近红外反射率降低,与侵染区差异明显,和实际情况相符。比较接种区和侵染区水稻平均反射率曲线,多光谱传感器不仅在可见光波段反映了较可见光传感器更强的差异,在红边和近红外波段差异更加明显,这说明专业窄波段传感器在病害监测方面较宽波段消费级传感器更有优势。

为寻求用于水稻纹枯病病害等级评估的最优图像植被指数,需先检验图像植被指数与地面实测 NDVI 的一致性。表 1 列出了七种可见光植被指数和三种多光谱植被指数,基于此计算两种传感器所获接种区和侵染区图像的多种植被指数。

选取决定系数(R<sup>2</sup>)、均方根误差(RMSE)、预测精度(Precision)作为模型精度的分析指标[见式(1)~式(3)]。

$$R^2 = \frac{\sum_{i=1}^n (P_i - P)^2 \times (Q_i - Q)^2}{\sum_{i=1}^n (P_i - P)^2 \sum_{i=1}^n (Q_i - Q)^2} \quad (1)$$

$$RMSE = \sqrt{\frac{1}{n} \sum_{i=1}^n (P_i - Q_i)^2} \quad (2)$$

$$Precision = \frac{1}{n} \sum_{i=1}^n \left( 1 - \text{abs} \left( \frac{P_i - Q_i}{Q_i} \right) \right) \quad (3)$$

式中, n 为样本量, i 为第 i 个样本, P<sub>i</sub>, P, Q<sub>i</sub>, Q 分别为预测值、预测均值、观测值和观测均值。

## 2 结果与讨论

### 2.1 基于实测 NDVI 的传感器效果对比

多种图像植被指数与地面 NDVI 实测值的相关性分析(见表 2)结果表明,基于多光谱传感器计算的图像 NDVI 与实测 NDVI 相关性最高。当水稻受感染时,叶片逐渐变黄,

绿色植被覆盖率下降,由于红光和近红外波段对颜色变化敏感,所以 NDVI 十分适合监测水稻纹枯病的病害严重程度。多光谱图像 RVI 也可较好地监测水稻生长情况,效果仅次于 NDVI。此外,依次对比每一植被指数下接种区和感染区的  $R^2$ ,不难发现接种区  $R^2$  均高于感染区,说明该时期感染区病害情况轻于接种区,并未完全感染,符合实际情况。

表 2 多光谱传感器图像植被指数与实测 NDVI 的相关性分析

Table 2 Correlation analysis of image-based VIs from multispectral sensor and ground-based NDVI

	Inoculation zone			Infection zone		
	Model	$R^2$	RMSE	Model	$R^2$	RMSE
NDVI	$y=0.916x-0.274$	0.914 <sup>a</sup>	0.024	$y=0.969x-0.328$	0.863 <sup>a</sup>	0.024
RVI	$y=2.565x+0.214$	0.898 <sup>b</sup>	0.075	$y=3.008x-0.095$	0.848 <sup>b</sup>	0.080
NDI	$y=0.773x-0.251$	0.868 <sup>c</sup>	0.026	$y=0.856x-0.321$	0.812 <sup>c</sup>	0.026
ExR	$y=-0.632x+0.342$	0.867	0.021	$y=-0.705x+0.402$	0.809	0.022
ExG-ExR	$y=1.494x-0.605$	0.866	0.051	$y=1.674x-0.747$	0.799	0.053
G*	$y=0.287x+0.246$	0.857	0.010	$y=0.323x+0.219$	0.782	0.011
ExG	$y=0.862x-0.263$	0.857	0.030	$y=0.970x-0.344$	0.782	0.032
R*	$y=-0.246x+0.420$	0.847	0.009	$y=-0.272x+0.444$	0.796	0.009
NDWI	$y=-0.154x+0.028$	0.495	0.013	$y=-0.132x+0.015$	0.304	0.013
B*	$y=-0.041x+0.334$	0.218	0.007	$y=-0.051x+0.338$	0.183	0.007

Note: a is the best result; b is the second result; c is the third result

表 3 可见光传感器图像植被指数与实测 NDVI 的相关性分析

Table 3 Correlation analysis of image-based VIs from visible light sensor and ground-based NDVI

	Inoculation zone			Infection zone		
	Model	$R^2$	RMSE	Model	$R^2$	RMSE
NDI	$y=0.328x-0.187$	0.875 <sup>a</sup>	0.011	$y=0.347x-0.216$	0.703 <sup>a</sup>	0.014
ExG-ExR	$y=0.702x-0.459$	0.868 <sup>b</sup>	0.024	$y=0.734x-0.515$	0.702 <sup>b</sup>	0.030
ExR	$y=-0.264x+0.296$	0.864 <sup>c</sup>	0.009	$y=-0.285x+0.323$	0.696	0.012
G*	$y=0.146x+0.279$	0.854	0.005	$y=0.150x+0.269$	0.688	0.006
ExG	$y=0.437x-0.163$	0.854	0.016	$y=0.449x-0.192$	0.688	0.019
R*	$y=-0.085x+0.411$	0.788	0.004	$y=-0.097x+0.423$	0.610	0.005
B*	$y=-0.061x+0.311$	0.530	0.005	$y=-0.053x+0.308$	0.303	0.005

Note: a is the best result; b is the second result; c is the third result

依次比较基于两种传感器获取两种区域的同种图像植被指数(NDI, ExR, ExG-ExR, G\*, ExG, R\*, B\*)与实测 NDVI 的决定系数(图 5)。结果表明,除 B\* 外,NDI, ExR, ExG-ExR, G\*, ExG, R\* 与实测 NDVI 基本属于高度相关。

接种区水稻病害较为严重,多光谱传感器和可见光传感器的监测效果没有显著差异,而在感染区,水稻病害感染相对较轻,此时多光谱传感器的监测效果更为精确灵敏。

从图 6 中可以看出,基于多光谱传感器计算的图像 NDVI 与实测 NDVI 拟合度最高,接种区  $R^2$  为 0.914, RMSE 为 0.024,感染区  $R^2$  为 0.863, RMSE 为 0.024。对于可见光传感器,NDI 与实测 NDVI 的相关性最好,接种区  $R^2$  为 0.875, RMSE 为 0.011,感染区  $R^2$  为 0.703, RMSE 为 0.014。因此,对于水稻纹枯病病害监测,多光谱图像 NDVI 可能有最好的效果。

可见光传感器波段数较少,波段较宽,并不是针对农业监测设计,仅能用于评估同一图像内植被的相对健康程度,对于水稻病害严重程度的评估效果相对较差。但其捕获的图像与人眼看到的图像相似,这意味着即使没有使用植被指数分析也可在一定程度上对图像进行解译,且价格低廉,是经

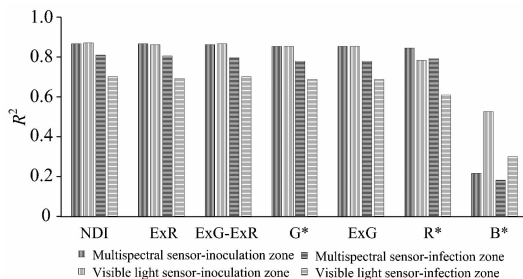


图 5 不同传感器不同区域同种植被指数比较  
Fig. 5 Comparison of the same VI from different sensors and zones

济的选择。多光谱传感器较可见光传感器而言,提供了农作物长势监测需要的红边、近红外等波段,但价格昂贵,不利于农业推广。因此,使用者应针对具体的应用需求,选择合适的传感器。

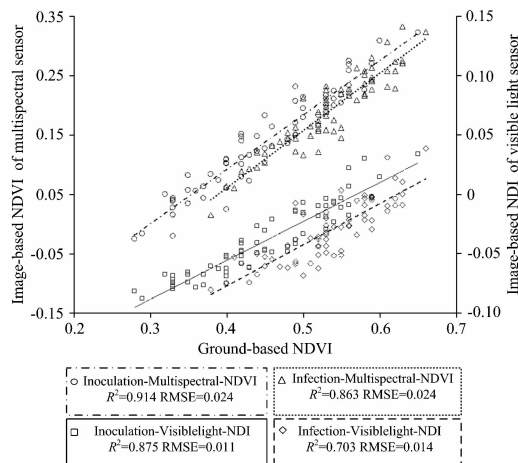


图 6 两种传感器最优图像植被指数效果对比

注:右轴为NDI刻度

Fig. 6 Effect comparison of optimal image-based

VI of two sensors

Note: the right axis is the scale of NDI

## 2.2 病害等级反演模型

由上述结论可知,对于多光谱传感器,图像NDVI与地面实测NDVI相关性最好,对于可见光传感器,图像NDI与地面实测NDVI相关性最好,分别基于这两种传感器的最优图像植被指数作为自变量反演水稻纹枯病病害等级,建立水稻纹枯病病害等级反演模型(图7)。

图7表明利用多光谱图像NDVI建立的反演模型, $R^2$ 达到0.624, RMSE为0.801,预测精度为90.04%,拟合度良好。利用可见光传感器图像NDI建立的反演模型, $R^2$ 为0.580,拟合度稍低于前者, RMSE为0.847,预测精度为89.45%,效果较差。根据图像NDVI与病害指数的散点图,可以看出两者间存在较好的线性趋势。极少数负NDVI值是存在的,这可能是因为样田中含有水分、土壤、枯萎的黄色茎叶。实际情况中,NDVI为负的样田,病害程度达到9级,植物结构和冠层颜色发生显著变化。综上,基于多光谱传感器NDVI建立的反演模型对于评估水稻纹枯病病害等级更精确。

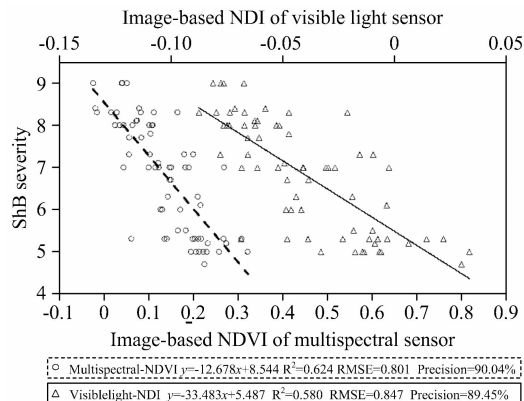


图 7 基于不同传感器的水稻纹枯病病害等级反演模型

注:顶轴为NDI刻度

Fig. 7 ShB severity inversion model based on different sensors

Note: the top axis is the scale of NDI

## 3 结论

基于无人机分别搭载可见光传感器和五波段多光谱传感器,对其图像和光谱进行分析,结合地面实测NDVI和病害指数数据,定量评估不同传感器所获接种区、侵染区的多种图像植被指数与实测NDVI之间的相关性,结果表明,多光谱传感器的NDVI与实测NDVI呈高度相关,接种区 $R^2$ 高达0.914, RMSE为0.024,侵染区 $R^2$ 为0.863, RMSE为0.024,效果最好。可见光传感器计算的NDI与实测NDVI得到了接种区 $R^2$ 为0.875, RMSE为0.011,侵染区 $R^2$ 为0.703, RMSE为0.014的结果。此外,在病害接种区,两种传感器对病害的监测效果相近,但在病害较轻的侵染区,多光谱传感器监测效果更为精确。最后利用多光谱图像NDVI反演水稻纹枯病的病害等级, $R^2$ 达到0.624,相关性较高, RMSE为0.801,预测精度为90.04%,拟合度良好,而利用可见光传感器图像NDI建立的反演模型, $R^2$ 为0.580, RMSE为0.847,预测精度为89.45%,效果稍差。综上,基于多光谱传感器获取的NDVI在水稻病害等级评估方面有较大的潜力。本研究采用的方法较为简单,成本较低,易于推广。后续研究将进一步优化飞行方案,挖掘所获图像的图谱信息,获取更多水稻生理生化指标,以科学快速地指导定量喷药,推动实现绿色植保的目标。

## References

- [1] Sumithra Muthayya, Jonathan D Sugimoto, Scott Montgomery, et al. *Annals of the New York Academy of Sciences*, 2014, 1324(1): 7.
- [2] Zhang Dongyan, Lan Yubin, Zhou Xingen, et al. In *Proceedings of 2015 ASABE Annual International Meeting*, New Orleans, Louisiana, USA, July 26-29, 2015.
- [3] Mosleh M K, Hassan Q K, Chowdhury E H. *Sensors*, 2015, 15(1): 769.
- [4] ZHANG Jing-cheng, YUAN Lin, WANG Ji-hua, et al (张竞成, 袁琳, 王纪华, 等). *Transactions of the Chinese Society of Agricultural Engineer*(农业工程学报), 2012, 28(20): 1.
- [5] ZHANG Dong-yan, SONG Xiao-yu, MA Zhi-hong, et al (张东彦, 宋晓宇, 马智宏, 等). *Scientia Agricultura Sinica*(中国农业科学),

- 2010, 43(11): 2239.
- [ 6 ] Anne-Katrin Mahlein. *Plant Disease*, 2016, 100(2): 241.
- [ 7 ] Matheus Kuska, Mirwaes Wahabzada, Marlene Leucker, et al. *Plant Methods*, 2015, 11(1): 28.
- [ 8 ] Elke Bauriegel, Werner B. Herppich. *Agriculture*, 2014, 4(1): 32.
- [ 9 ] Qin Zhihao, Zhang Minghua. *International Journal of Applied Earth Observation & Geoinformation*, 2005, 7(2): 115.
- [10] Faranak Ghobadifar, Aimrun Wayayok, Shattri Mansor, et al. *Geomatics, Natural Hazards and Risk*, 2016, 7(1): 237.
- [11] Zhou X, Zheng H B, Xu X Q, et al. *ISPRS Journal of Photogrammetry and Remote Sensing*, 2017, 130: 246.
- [12] Jia Yinjiang, Su Zhongbin, Shen Weizheng, et al. *International Journal of Smart Home*, 2016, 10(5): 159.
- [13] Ballesteros R, Ortega J F, Hernández D, et al. *Precision Agriculture*, 2014, 15(6): 579.
- [14] Zhang Jian, Yang Chenghai, Song Huaibo, et al. *Remote Sensing*, 2016, 8(3): 257.
- [15] Sankaran Sindhuja, Maja Joe Mari, Buchanon Sherrie, et al. *Sensors*, 2013, 13(2): 2117.

## Comparison between the Effects of Visible Light and Multispectral Sensor Based on Low-Altitude Remote Sensing Platform in the Evaluation of Rice Sheath Blight

ZHAO Xiao-yang<sup>1, 2</sup>, ZHANG Jian<sup>1, 2\*</sup>, ZHANG Dong-yan<sup>3</sup>, ZHOU Xin-gen<sup>4</sup>, LIU Xiao-hui<sup>3</sup>, XIE Jing<sup>5\*</sup>

1. College of Resources and Environment, Huazhong Agricultural University, Wuhan 430070, China

2. Key Laboratory of Farmland Conservation in the Middle and Lower Reaches of the Ministry of Agriculture and Rural Affairs, Wuhan 430070, China

3. Anhui Engineering Laboratory of Agro-Ecological Big Data, Anhui University, Hefei 230601, China

4. Texas A&M AgriLife Research and Extension Center, Beaumont, TX 77713, USA

5. College of Science, Huazhong Agricultural University, Wuhan 430070, China

**Abstract** Efficient and non-destructive assessment of crop disease grade is of great significance to the practical agricultural production and research. In this study, the feasibility of low-altitude UAV (Unmanned Aerial Vehicle) remote sensing platform for the disease grade assessment of rice Sheath Blight (ShB) was discussed. Then the spectral response differences of visible light sensor and multispectral sensor and their effects on the spectral reflectance acquisition of rice with ShB were analyzed. And rice ShB monitoring effects of two kinds of sensors were compared quantitatively. The study area consisted of 67 rice plots with different varieties, each of which was divided into inoculation zone and infection zone. The drone was Phantom 3 Advanced, a small consumer-grade UAV made by DJI-Innovations company, and the payloads were the self-contained visible light sensor and Micasense RedEdge<sup>TM</sup> multispectral sensor to acquire remote sensing images respectively. At the same time, the rice ShB disease grades were investigated by manual expert recognition and measured NDVI was obtained with Trimble's GreenSeeker<sup>®</sup> Handheld Crop Sensor. Remote sensing images were preprocessed by image mosaic, layer stacking and radiometric calibration. A total of 134 plots in inoculation and infection zones of visible light image were used to calculate seven kinds of visible light vegetation indices, namely NDI (Normalized Difference Index), ExG (Excess Green), ExR (Excess Red), ExG-ExR, B\*, G\* and R\*. Besides the above seven kinds of visible light vegetation indices, multispectral image was calculated by three kinds of multispectral vegetation indices additionally, namely NDVI (Normalized Difference Vegetation Index), RVI (Ratio Vegetation Index) and NDWI (Normalized Difference Water Index). The correlation between the image-based vegetation index and ground-based NDVI was analyzed, and the optimal image-based vegetation indices of the visible light and multispectral sensor were selected to establish the disease grade inversion model of rice ShB. The results of correlation analysis showed that the fitting degree of image-based NDVI and ground-based NDVI based on multispectral sensor was the highest, and  $R^2$  was 0.914 and RMSE was 0.024 in the inoculation zone, while  $R^2$  and RMSE were 0.863 and 0.024 respectively in the infection zone. As for the visible light sensor, the correlation between image-based NDI and measured NDVI was best, and  $R^2$  was 0.875 and RMSE was 0.011 in the inoculation zone, while  $R^2$  was 0.703 and RMSE was 0.014 in the infection zone. The consistencies of the same image-based vegetation index and ground-based NDVI of two kinds of sensors and two kinds of zones were compared, which revealed that NDI, ExR, ExG-ExR, G\*, ExG, R\* except B\* were mainly highly correlated with the measured NDVI. In the inoculation zones with severe disease, the two kinds of sensors had similar effects on the detection of rice ShB, but the monitoring effect of multispectral sensor was more precise and sensitive in infection zones with relatively lighter disease. The disease grade inversion model

of rice ShB established by NDVI based on multispectral sensor was effective, whose  $R^2$  reached 0.624, and RMSE was 0.801 and prediction accuracy was 90.04%. The disease grade inversion model established by NDI based on visible light sensor was slightly worse, whose  $R^2$  was 0.580, and RMSE was 0.847 and prediction accuracy was 89.45%. The spectral response curves of visible light and multispectral sensor were compared and analyzed. The visible light sensor can obtain three bands of red, green, blue in the range of visible light, and wavelength range overlaps with each other, while the multispectral sensor including five imaging units can independently obtain five narrow-band spectral bands from visible light to near infrared providing subtler spectral information. Through comparing the average reflectance curves of rice in inoculation zone and infection zone, the multispectral sensor not only reflected bigger difference than visible light sensor in the visible light band, but also represented more obvious difference in the red and near infrared band, which demonstrated that the professional narrow-band sensor had an advantage over broad-band consumer-grade sensor in the rice ShB monitoring. In conclusion, it is feasible to evaluate the disease grade of rice ShB based on the low-altitude UAV remote sensing platform with visible light and multispectral sensor. The multispectral sensor is precise and sensitive which can be used for early detection of rice ShB, and the visible light sensor is less accurate but economical and easy to popularize. The results of this study are expected to provide decision support for diseases control and be beneficial to promoting precision agriculture and ensuring food security.

**Keywords** Visible light sensor; Multispectral sensor; Low-altitude remote sensing; Rice sheath blight; Disease grade evaluation; Vegetation index

(Received Jan. 15, 2018; accepted May 20, 2018)

\* Corresponding authors